HNUE JOURNAL OF SCIENCE
Natural Sciences 2025, Volume 70, Issue 1, pp. 44-52
This paper is available online at http://hnuejs.edu.vn/ns
DOI: 10.18173/2354-1059.2025-0006

PHONON DYNAMICS AND OPTICAL PROPERTIES OF WURTZITE CdS

Nguyen Minh Hoa
Faculty of Fundamental Sciences, Hue University of Medicine and Pharmacy, Hue University, Hue city, Vietnam
Corresponding author: Nguyen Minh Hoa, e-mail: nguyenminhoa@hueuni.edu.vn

Received January 3, 2025. Revised March 22, 2025. Accepted March 31, 2025.

Abstract. This study provides a comprehensive investigation of the structural, vibrational, optical, and thermodynamic properties of wurtzite cadmium sulfide (CdS) using computational methods. Using density functional theory (DFT) and phonon analysis, we reveal stable phonon dispersion with distinct acoustic and optical modes. The phonon density of states (PDOS) highlights the contributions of cadmium and sulfur sublattices, with key modes identified at 34.7 cm^{-1}, 124.4 cm^{-1}, 273 cm^{-1}, and 305.5 cm^{-1}. Optical analysis shows that CdS is transparent below 3.5 eV, exhibiting a maximum refractive index of 2.96 at 3.05 eV, and strong absorption at 7.76 eV (with an extinction coefficient of 1.88). Thermodynamic analysis indicates decreasing entropy and Gibbs free energy with rising temperature. The vibrational zero-point energy (ZPE) is calculated to be 0.124 eV, which is consistent across different calculation methods. These results provide valuable insights into the fundamental properties of CdS for its use in optoelectronic applications.

Keywords: cadmium sulfide, wurtzite, phonon density of states, thermodynamic, DFT.

1. Introduction

Cadmium sulfide (CdS), a versatile semiconductor, exhibits two primary crystal structures: zinc blende (ZB) and hexagonal wurtzite (WZ), with the final structure depending on synthesis conditions [1]-[3]. Although both phases are generally stable, CdS transitions to a rock salt phase and then a β-Sn phase under high pressure [4]. Due to its favorable electronic and optical properties, CdS is extensively investigated for applications in optoelectronic devices, including solar cells, light-emitting diodes, and photodetectors [5]. Optimizing CdS's performance in these devices necessitates a deep understanding of its electronic, vibrational (phonon), optical, and thermodynamic properties. This knowledge gap underscores the importance of continued research to further refine CdS for these and other potential applications [5]-[7].

Furthermore, the room-temperature band gap of approximately 2.42 eV makes CdS a promising material for nonlinear optical applications [5]. Its strong covalent bonding allows for the growth of large, stable single crystals, while its relatively low birefringent walk-off angle makes it suitable for diverse optical uses [8]. Although much research has focused on CdS's optical behavior in the visible and near-infrared regions, its properties in other spectral ranges, particularly concerning its fundamental material characteristics, warrant further investigation.

Despite extensive theoretical studies on the electronic and phonon band structures of CdS, especially in the WZ phase, there remains a notable gap in understanding the temperature-dependent behavior of key thermodynamic parameters, such as the Debye temperature, and the Raman spectra of WZ CdS [9]. While the phonon band structures and thermodynamic properties of CdS in the zinc blende (ZB) phase are well-documented, its behavior in the WZ phase, particularly concerning phonon dynamics and related thermodynamic characteristics, requires further attention [5], [10].

Therefore, this study aims to provide a detailed computational analysis of the optical and thermodynamic properties of WZ CdS. Specifically, we investigate the refractive index and extinction coefficient to enhance our understanding of CdS's optical behavior in the WZ structure. Furthermore, using density functional theory (DFT), we calculate the vibrational modes to gain insights into its intrinsic phonon dynamics. We also explore the temperature-dependent phonon and thermodynamic properties of WZ CdS using the generalized gradient approximation (GGA) with the Perdew-Burke-Ernzerhof (PBE) functional. This comprehensive study seeks to contribute valuable knowledge, illuminating CdS's potential for a range of applications.

2. Content

2.1. Theoretical calculation

2.1.1. CdS structure

CdS typically adopts a hexagonal WZ structure, characterized by the $P6_3mc$ space group symmetry [11]. The primitive cell contains two Cd-S pairs, with each Cd atom tetrahedrally coordinated by four S atoms and vice versa. Experimentally determined lattice parameters for the primitive cell are: $a = b = 4.16$ Å, $c = 6.72$ Å, $\alpha = \beta = 90°$, $\gamma = 120°$, with space group $P6_3mc$. A 2×2×2 CdS supercell, illustrated in Figure 1, was constructed from this primitive cell for our calculations. It is worth noting that CdS can exist in three distinct structural forms, each with unique structural parameters.

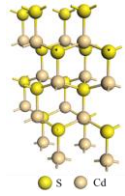

Figure 1. Crystal structure of WZ CdS

2.1.2. Theoretical calculation

In this study, we calculated the phonon dispersion spectra and the projected phonon density of states (PDOS) of CdS crystals using density functional perturbation theory. First-principles calculations were performed using the plane-wave pseudopotential method, as implemented in the CASTEP package [12], [13]. The exchange-correlation functional was modeled using the GGA with the PBE functional [13]. Ion–electron interactions were treated with optimized norm-conserving pseudopotentials. A kinetic energy cutoff of 450 eV and a Monkhorst–Pack k-point mesh with a density less than 0.07/Å^3 in the Brillouin zone were employed for structural relaxation and electronic structure calculations. To obtain the phonon dispersion, the linear response method was used. For these calculations, a kinetic energy cutoff of 1000 eV and a Monkhorst–Pack k-point grid with a spacing less than 0.07/Å were utilized. The lattice parameters and atomic positions were fixed based on experimental values for all calculations.

2.2. Results and discussion

2.2.1 Phonon dispersion

The computed phonon dispersion and density of states (DOS) for wurtzite CdS reveal crucial insights into the material's vibrational dynamics and stability. The wurtzite structure (space group $P6_3mc$, C_{6v} symmetry), with four atoms per unit cell, gives rise to nine optical phonon branches at the Brillouin zone center. These include A_1 and E_1 modes (both Raman and infrared active), E_2 modes (Raman active), and B_1 modes (optically inactive). Due to electric field effects, the polar A_1 and E_1 modes exhibit transverse optical (TO) and longitudinal optical (LO) phonon splitting [14]. As shown in Figure 2, the calculated phonon dispersion along the high-symmetry path (Γ-A-H-K-Γ-M-L-H) within the Brillouin zone confirms the dynamic stability of the WZ structure, as all phonon frequencies remain positive. The analysis reveals a clear separation between the optical (LO and TO) and acoustic (LA and TA) modes, further characterizing the material's unique vibrational properties.

The high-symmetry point coordinates are as follows: Γ(0,0,0); A(0,0,0.5), H(-0.333,0.667,0.5), K(-0.333,0.667,0), M(0,0.5,0), and L(0,0.5,0.5). Phonon dispersion analysis is essential for evaluating material stability, identifying material phases, and guiding synthesis and applications. The acoustic branches represent overall vibrations of the crystal lattice, while optical branches signify relative atomic vibrations within the unit cell. The vibration frequency (ω) is influenced by the elastic constant (β), representing the material's stiffness; the interaction energy between atoms ($E(x)$); the displacement (x) of atoms from their equilibrium positions, and the atomic mass (m). These parameters are related by the following equation [15]:

$$\omega = \sqrt{\frac{\beta}{m}} = \sqrt{\frac{1}{m}\frac{\partial^2 E(x)}{\partial x^2}} \ .$$

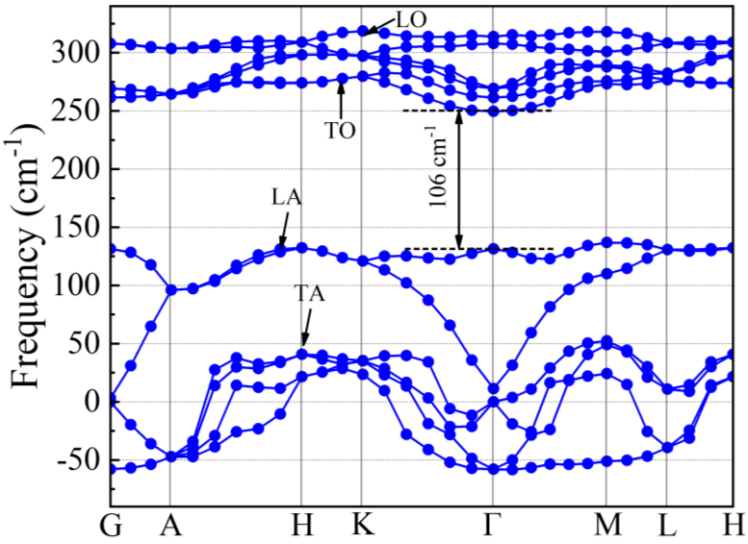

Figure 2. The calculated phonon dispersion of WZ CdS

The PDOS analysis, depicted in Figure 3, provides significant insights into the vibrational dynamics of wurtzite CdS. At lower frequencies (below 150 cm^{-1}), the DOS is dominated by acoustic modes, primarily involving collective vibrations of the heavier cadmium (Cd) sublattice. In contrast, the higher-frequency region is dominated by optical modes, primarily due to the relative vibrations within the lighter sulfur (S) sublattice. A band gap at approximately 106 cm^{-1} separates these optical modes into two distinct regions: vibrations below this gap are primarily attributed to Cd atom displacements, while those above it are predominantly associated with S atom displacements. Specifically, prominent vibrational modes were identified at 34.7 cm^{-1} (E_1 mode, corresponding to vibrations perpendicular to the c-axis), 124.4 cm^{-1} (A_1 mode, representing vibrations along the c-axis), 273 cm^{-1} (E_2 mode, corresponding to vibrations in the basal plane), and 305.5 cm^{-1} (B_1 mode) [10], [16]. These calculated mode frequencies, obtained using GGA calculations, are consistent with previous theoretical studies, validating our approach and providing a comprehensive understanding of the vibrational properties and stability of WZ CdS.

While our phonon dispersion results align with prior studies, our detailed analysis of the sublattice contributions to the PDOS provides new insights into the vibrational dynamics of wurtzite CdS. Specifically, we identify distinct frequency regions dominated by Cd and S vibrations, separated by a band gap at approximately 106 cm^{-1}. Furthermore, our exploration of temperature-dependent phonon behavior and its impact on thermodynamic properties offers a deeper understanding of the material's stability and performance in practical applications. These findings, combined with our integrated analysis of optical and thermodynamic properties, contribute novel insights to the field and underscore the potential of wurtzite CdS for optoelectronic applications.

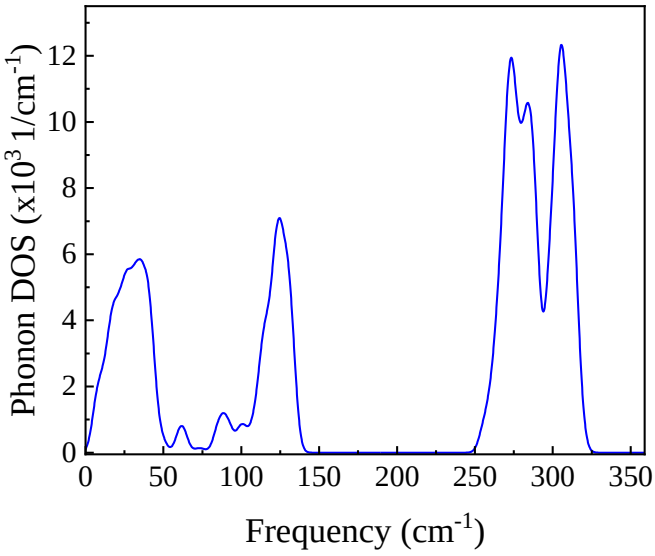

Figure 3. The calculated phonon density of states of WZ CdS

2.2.2. Optical properties

The optical properties of WZ CdS were investigated through an analysis of the refractive index (*n*) and extinction coefficient (*k*), as presented in Figure 4. These parameters are essential for understanding how CdS interacts with light, which is crucial for its optoelectronic applications. The refractive index (*n*) determines how much light bends as it passes through a material, while the extinction coefficient (*k*) indicates the extent of light absorption at different wavelengths.

The spectral analysis of *n* and *k* for WZ CdS revealed notable features. Specifically, at photon energies below 3.5 eV, CdS exhibits low absorption, consistent with the band gap of ~2.4 eV, as experimentally confirmed by Ward [17]. The refractive index reaches a maximum value of 2.96 at 3.05 eV, indicating that light will transmit through the material with minimal bending. At lower photon energies, ranging from 1.57 to 3.7 eV, the refractive index varies considerably before decreasing rapidly as photon energy increases. The extinction coefficient (*k*) displays a broad peak around 7.76 eV with a maximum value of 1.88, indicating strong absorption within this spectral range. This behavior is consistent with the experimental findings of Yoshikawa and Sakai, who reported similar trends in the optical properties of wurtzite CdS [18].

This behavior can be strategically leveraged in the design of CdS-based optoelectronic devices. For example, the transparency of CdS makes it an excellent candidate for use as a window layer in thin-film solar cells, enabling efficient light transmission to the absorber layer. In light-emitting diodes (LEDs), CdS can serve as a transparent electrode or waveguiding layer, directing emitted light toward the desired output. Additionally, the material's transparency in the visible range makes it suitable for visible-blind photodetectors and optical coatings, such as anti-reflective coatings and bandpass filters.

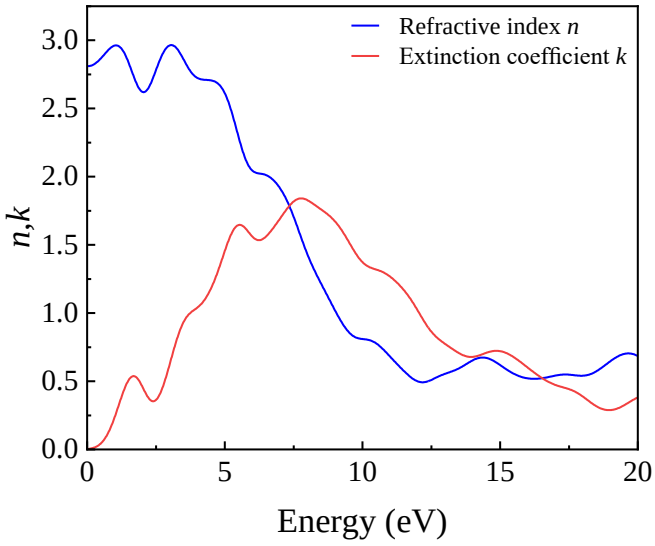

Figure 4. Theoretically calculated spectra of the refractive index (n) and extinction coefficient (k) for WZ CdS

2.2.3. Thermodynamic behavior

The temperature-dependent structural stability of CdS in the WZ phase was investigated by calculating its thermodynamic properties up to 1000 K. As expected, our results show a decrease in entropy (*S*) and Gibbs free energy (*G*) with rising temperature, consistent with prior studies [19]. This calculation was performed using the PDOS derived from the quasi-harmonic approximation and the GGA method. The calculated thermodynamic parameters enthalpy (*H*), entropy (*S*), and Gibbs free energy (*G*) are illustrated in Figure 5. As the temperature increases, a notable decrease in entropy (*S*) is observed. This decrease is attributed to a reduction in the PDOS at lower frequencies, leading to a decrease in vibrational entropy, as defined by the equation [10]: $S = k_B \ln \Omega$, where k_B is Boltzmann's constant, Ω represents the number of microstates for a given configuration. Analysis of the phonon DOS curves reveals that the dominant peak associated with the optical phonon modes shifts toward lower frequencies as temperature increases. This shift reflects the influence of atomic mass on vibrational characteristics, consistent with the WZ structure of CdS and its lighter anionic mass compared to its heavier cationic mass. The Gibbs free energy (*G*), significantly influenced by vibrational entropy, also decreases with increasing temperature, in line with established thermodynamic principles. The temperature dependence of thermodynamic properties, such as S and G, provides critical insights into the long-term stability and performance of CdS under operational conditions. Our calculations show that entropy decreases with increasing temperature, reflecting a reduction in the phonon density of states (PDOS) at lower frequencies. This behavior indicates that the material

becomes more ordered at higher temperatures, as the vibrational modes soften and the system settles into a more stable configuration.

Similarly, Gibbs free energy decreases with increasing temperature, indicating that the material becomes more thermodynamically stable at higher temperatures. This behavior is consistent with the expected properties of wurtzite CdS and has important implications for its use in practical applications. For example, the decreasing Gibbs free energy suggests that CdS can maintain its structural integrity and performance under thermal stress, making it suitable for use in high-temperature environments such as solar cells, thermoelectric devices, and catalysis.

Furthermore, the calculated vibrational zero-point energy (ZPE), a critical factor in molecular energetics, was determined using the equation [6]: $E_{vib}(0) = \frac{1}{2} h \sum_i \nu_i$, where ν_i refers to the normal-mode vibrational frequencies. The ZPE value for CdS, as determined using the GGA, was found to be 0.124 eV, which is consistent with previous theoretical studies, validating our computational approach. While the thermodynamic trends themselves may not be novel, our integrated analysis of phonon dynamics, optical properties, and thermodynamic behavior offers a more comprehensive understanding of CdS's material properties and their implications for optoelectronic applications.

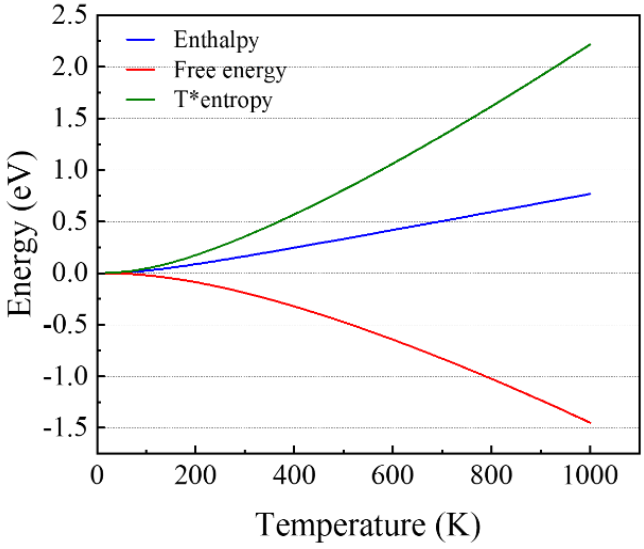

Figure 5. Calculated temperature dependence of Gibbs free energy (G), enthalpy (H), and entropy (S) for WZ CdS

3. Conclusions

Our detailed computational study of WZ CdS provides a comprehensive understanding of its properties, encompassing vibrational, optical, and thermodynamic behavior. We confirmed the dynamic stability of the material through phonon dispersion calculations, identified unique features in the DOS, and determined specific vibrational

mode frequencies and sublattice contributions. Analysis of the optical properties highlighted its potential for light manipulation. Furthermore, the thermodynamic behavior at temperatures up to 1000 K reveals the material's structural changes and energy considerations, such as ZPE, offering important data for device optimization. The calculated results of these multiple analyses show strong agreement with previous theoretical studies. These findings underscore the potential of WZ CdS in a wide range of applications, especially in optoelectronics, and pave the way for future experimental investigations and further development in advanced energy materials.

REFERENCES

[1] Nguyen MH, Le DT, Pham VD & et al., (2024). Fine-tuning bandgap, lifetime, and phonon characteristics in CdSe nanocrystals for enhanced optoelectronic device applications. *Journal of Materials Science: Materials in Electronics*, 35(26), 1756.

[2] Hu R, He F, Hou R & et al. (2024). The Narrow Synthetic Window for Highly Homogenous InP Quantum Dots toward Narrow Red Emission. *Inorganic Chemistry*, 63(7), 3516-3524.

[3] Chopade P, Jagtap S & Gosavi S, (2022). *Material Properties and Potential Applications of CdSe Semiconductor Nanocrystals.* Nanoscale Compound Semiconductors and their Optoelectronics Applications, p. 105-153.

[4] Kashuba AI, Andriyevsky B, Semkiv IV & et al., (2022). Calculation of the vibrational spectra of CdSe and CdS crystals with zinc blende structure. *Materials Today: Proceedings*, 62 (9), 5812-5818.

[5] Güler E, Uğur, Güler M, et al., (2024). Theoretical Predictions for Elastic, Mechanical, Anisotropic, Electronic, and Optical Profiles of Wurtzite CdS, CdSe, and CdTe. *Jom*, 77(4), 1-10.

[6] AlGhamdi GS, Saini A & Kumar R, (2023). Electronic, Elastic, and Thermoelectric Properties of Bulk CdX (X = S, Se, and Te) Binary Semiconductors from First-Principles Approaches. *Physica Status Solidi (B): Basic Research*, 260(7), 2300012.

[7] Sun C, Zhang C & Zhang B, (2022). Adjusting the structural, electronic and optical properties of CdS by the introduction of Be: A DFT study. *Materials Today Communications*, 31, 103394.

[8] Wu L, Li Y, Liu GQ & et al., (2024). Polytypic metal chalcogenide nanocrystals. *Chemical Society Reviews*, 53, 9832-9873.

[9] Ed-Dahmouny A, Althib HM, Arraoui R, Jaouane M, El-Bakkari K, Fakkahi A, Azmi H, Mazouz A, Jaafar M, Zeiri N, Saadaoui S, Sali A, (2025). Tunable energy spectrum and enhanced absorption in doped CdS/ZnSe spheroidal core/shell quantum dots under the magnetic field. *Computational Materials Science*, 250, 113720.

[10] Musari AA, Joubert DP & Adebayo GA, (2019). DFT investigation of elastic, mechanical, vibrational, and thermodynamic properties of cadmium dichalcogenides. *Physica B: Condensed Matter*, 552, 159-164.

[11] Biswas A, Meher SR & Kaushik DK, (2022). Electronic and Band Structure calculation of Wurtzite CdS Using GGA and GGA+U functionals. *Journal of Physics: Conference Series*, 2267(1), 012155.

[12] Monkhorst HJ & Pack JD, (1976). Special points for Brillouin-zone integrations. *Physical Review B*, 13(12), 5188-5192.

[13] Perdew JP, Ruzsinszky A, Csonka GI & et al., (2008). Restoring the density-gradient expansion for exchange in solids and surfaces. *Physical Review Letters*, 100(13), 039902.

[14] Fu J, Chen S & Liu X, (2022). Calculation of lattice vibrational and thermal properties of cadmium sulfide nanocrystal and growth preference of cadmium sulfide powder during microwave-hydrothermal process. *International Journal of Quantum Chemistry*, 122(2), e26828.

[15] Ingle RV, Shaikh SF, Kaur J & et al., (2023). Optical and Electronic Properties of Colloidal Cadmium Sulfide. *Materials Science and Engineering: B*, 294, 116487.

[16] Yan D, Xu D, Li J & et al., (2018). Terahertz optical properties of nonlinear optical CdSe crystals. *Optical Materials*, 78, 484-489.

[17] Oncan N, Ward L & Player MA, (1994). The optical properties of thin erbium films. *Optics and Laser Technology*, 26(5), 361-364.

[18] Akihiko Yoshikawa and Yoshio Sakai (1974), Optical Properties of Hetero-Epitaxial CdS Films. *Japanese Journal of Applied Physics*, 13 *13*(9), 1353.

[19] Edossa TG & Woldemariam MM, (2022). Study of dynamic and thermodynamic properties of zinc-blend and wurtzite cadmium sulfide (CdS) using density functional theory. *Zeitschrift für Naturforschung A*, 77(2), 171-179.